E6-2001-93

J.Adam[1], J.Dobeš[2], M.Honusek[2], V.G.Kalinnikov,
J.Mrázek[2], V.S.Pronskikh[3], P.Čaloun[1], N.A.Lebedev,
V.I.Stegailov, V.M.Tsoupko-Sitnikov

GAMMA-RAYS AND E0 AND M1+E0 TRANSITIONS IN ^{152}Tb $\rightarrow$ ^{152}Gd DECAY

[1]On leave from: Nuclear Physics Institute of ASCR, Řež,
Chech Republik
[2]Nuclear Physics Institute of ASCR, Řež, Czech Republik
[3]St.Petersburg State Institute of Technology, Russia

1 Introduction

The nucleus $^{152}_{65}Tb_{87}$ ($I^{\pi} = 2^-$) decays via EC/β+ to the excited states and the ground state of the even-even stable nucleus $^{152}_{64}Gd_{88}(I^{\pi} = 0^+)$. The $^{152}_{65}Tb_{87}$ half-life is 17.5(1) h, its β-decay energy is Q_{β} = 3850(15) keV. This nucleus is at the limits of the region of nuclear deformation, consequently the origin of its excited states may refer to that of either spherical or weakly deformed nuclei as well as its wave-function may be presented as a mixed state of these two types. One can also expect the nuclei belonging to the transitional region (between spherical and deformed ones) to feature an E0-multipolarity admixture to M1+E2-transitions between the levels of identical non-zero spin. Properties of the excited levels with energies from 0 keV up to 1500-2000 keV have been studied quite well whereas the experimental data for the higher-energy levels are not so complete. Rather detailed data on the intensities of internal conversion electrons from this decay were previously published in [1], where the measurements were carried out in two energy regions : below 1000 keV with an orange-type spectrometer ($\Delta(H\rho)/H\rho$ = 0.4%) and above 900 keV with a two-fold double-focussing $2\pi\sqrt{2}$-type spectrometer ($\Delta(H\rho)/H\rho = 0.21\%$). The latest results of the single γ-ray and $\gamma\gamma$-coincidence measurements were published in [2].

2 Measurement of single γ-rays

A tantalum target was irradiated by an internal proton beam (E_p=660 MeV, I_p=5$_{\mu}$A) of the LNP Phasotron and a radioactive source of ^{152}Tb was prepared from it by means of chromatographic isolation followed by electromagnetic separation.

Gamma-rays from the ^{152}Tb decay were measured in the energy range from 5 keV to 1500 keV with a planar HPGe detector ($\oslash$12 mm, thickness 5 mm) with the energy resolution $\Delta E_{\gamma} = 350\ eV$ for $E_{\gamma} = 6.9\ keV$ and with a coaxial HPGe detector (ε=19% and ΔE_{γ}=1.8 keV (^{60}Co). In measurements with the coaxial detector a 1 mm Cu + 1 mm Cd filter was used and the source-to-detector distance was d=80 mm.

In the higher-energy range (300-4000 keV), γ-quanta were recorded with another coaxial HPGe detector ($\varepsilon = 28\%$, $\Delta E_\gamma = 1.9\ keV$ (^{60}Co)). In the latter measurements a 1 mm Cu+2 mm Cd+7 mm Pb filter was mounted on the detector and the source-to-detector distance was set to 10 mm. Assignment of gamma peaks to the ^{152}Tb decay was based on their intensity fall with time, the background peaks and the peaks from other Tb isotopes were taken into consideration. Gamma quanta from the neighbouring isotopes ^{151,153,154}Tb were also observed in the spectra. Their activity contributed from 10^{-3} to 10^{-5} of the ^{152}Tb activity.

Transition energies in the ^{152}Tb decay were determined by the "internal calibration" approach : the ^{152}Tb source and a standard source of nearly equal intensities were placed at the same strictly defined distance of 10 mm from the detector. The γ-radiation was recorded in a broad energy range with a multichannel analyser SPECTRUM MASTER 919 (ORTEC) as 16384-channel spectra. The spectra were handled by the computer code DEIMOS [3], the initial parameters of fit were chosen interactively. Slight non-Gaussian variation in the shape of the high-intensity peaks was taken into account by insertion of an additional peak into the left slope of the main one. This dependence of a peak position in a spectrum on the processing method (the number of gaussians inserted in the peak) was thoroughly studied and the results are shown in Table 1.

Energies of ^{56}Co and ^{154}Eu γ-lines for the calibration purposes were taken from [4] while those of ^{226}Ra from [5], and energies of the 344.2785(13), 411.1165(13), 778.9045(24), 1089.737(5) and 1299.140(9) keV γ-transitions also taking place in ^{152}Eu decay were taken from [4]. Those γ-ray energies which had been measured with the planar detector were determined with the help of the following Standartized Radioactive Gamma-Ray Sources : ^{57}Co, ^{133}Ba, ^{152}Eu [4]. Purity of the "calibrating" peaks in the measurements of the ^{152}Tb decay in the presence of a standard source was checked by comparison of their intensities in our spectra to adopted ones. Using this approach we were able to reject some peaks from the channel-energy dependence. We expressed this dependence in a polynomial form of the 1st, 2nd and

3rd power and fitted them consecutively. The fitted residuals are given in Table 2 and Fig. 1. Differences of these polynomials are presented in Fig.2. For the 2nd(3rd) power polynomials these differences are as large as 170 eV (240 eV). We chose to use a 2nd power polynomial in all the data processing. The averaged energy residual from three measurements was found to be 70 eV. Of the 5 transitions also manifesting themselves in the ^{152}Eu decay, the 1089.737 keV transition was rejected because of presence of the relatively close to energy intense 1087.12 keV transition from the ^{152}Tb decay. On the basis of the "internal calibration" approach 24 transitions were chosen for further use, see Table 3. Their energies were taken as the averaged value of three independent measurements. The uncertainties were increased so that they became 70 eV larger than the doubled standard deviation to take into account the systematic error caused by the Gaussian-like expression for the peak shape ($\chi^2 > 1$, see Table 1) and the electric circuit non-linearity expression by the 2nd power polynomial. Thus, the γ-ray energy uncertainities used by us were

$$\sigma_{adopt}(E_\gamma) = \sqrt{4\sigma^2(E_\gamma) + (0.07)^2} \qquad [\text{keV}]$$

The main part of the ^{152}Gd excited level scheme was built on 86 transitions that had been observed in $\gamma - \gamma$-coincidencies [2], while 5 of those transitions were close in energy double transitions, energies of which were difficult to determine. The remaining 81 transitions were placed between 43 levels, and energies of the levels were determined by least squares fitting. We obtained $\chi^2 = 1.19$ for a set of 77 transitions, which can prove correctness of E_γ and ΔE_γ determination. We also unambiquously placed 87 more transitions between a set of 45 levels using the energy balance condition $\left[(E_i - E_k)_{(lev)} - E_\gamma(k)_{(tr)}\right] \leq 2\sigma$. We tried to determine intensities of the γ-transitions precisely. In particular, a thorough analysis of ballast peaks, namely, sum peaks, single and double escape peaks, was done. Energies and intensities of those peaks were calculated with the programs described in [6]. For example, a diversity of peaks of different origin measured in the range from 900 to 4000 keV on a detector equipped with a thick filter versus their intensities are given in Table 4. In the spectrum one can observe peaks

with intensities that exceed $S_\gamma^{(lim)}(E_\gamma)$,

$$S_\gamma^{(lim)}(E_\gamma) = \frac{3}{2}(FWHM)\sqrt{N(E_\gamma)}, \quad (1)$$

where $N(E_\gamma)$ is the number of counts registered in the spectrum at E_γ. In this energy range we observed 661 peaks, 62 of which were recognized as ballast and 331, identified as full-energy peaks, were corrected for a ballast admixture $S_\gamma(BP(E_\gamma))$, BP means ballast peak. In some cases these corrections were rather substantial, see Table 4, where the amount of corrected ^{152}Tb lines is shown versus intensities of their admixtures. Note that intensities of the 1048.1, 1123.3, 1343, 1353 and 2966 keV transitions (see ref.[2]) are completely equal to those of the ballast peaks. Substraction of a ballast peak intensity out of a full energy peak's one introduced additional uncertainity in energy of the latter peak. The summary of γ-rays corresponding to the decay of ^{152}Tb is given in Table 6.

3 Multipolarities of transitions

Relative intensities of internal conversion electrons (ICE) from the K-shell were taken from [1] where the measurements of [7] had been completed and made more precise. The ICE measurements were carried out with an orange-type β-spectrometer ($\Delta H\rho/H\rho = 0.4\%$, $\varepsilon \approx 1\%$) in the low-energy range and with a two-fold double-focussing $2\pi\sqrt{2}$-type low-background spectrometer ($\Delta H\rho/H\rho = 0.21\%$, $\varepsilon \approx 0.1\%$) in the high-energy range, as described above. Both spectra were "sewn together" to a common scale by the K615 keV line with a 15% uncertainty. This uncertainty was than neglected, as well as the uncertainty in the $2\pi\sqrt{2}$-spectrometer registration efficiency ($\Delta\varepsilon$(EC)=10%) at the K615 line [6]. The energy E_e [keV] and momentum ($H\rho$) of ICE are known to be connected by the relation :

$$\frac{\Delta E_e}{E_e} = \left(1 + \frac{511}{511 + E_e}\right)\frac{\Delta H\rho}{H\rho}.$$

Thus, the resolution of the HPGe detectors is better than that of the β-spectrometers. That is why some of the conversion lines should be con-

sidered as being complex (see below). On the basis of previous investigations of the ^{152}Tb decay scheme, some intense transitions were surely assigned either $E2$ or $E1$ multipolarities. The coefficient k, needed to connect I_K and I_γ internal units, was determined separately in both the low-energy region, using the 344 (E2), 411 (E2) and 778 keV (E1) ($k = 0.101(4)$) transitions, and the high-energy one (> 900 keV), using the 970(E1), 990(E2), 1185(E2), 1209(E1), 1299(E1), 1314(E1), 1941(E2), 2033(E1) and 2113 keV (E2) ($k = 0.0856(66)$), see Fig. 3. We determined this k by comparison of the experimental and theoretical K-shell conversion coefficients (α_K), i.e., $k\frac{I_K(E_i)}{I_\gamma(E_i)} = \alpha_K^{theo}(E_i(XL))$, where XL are transition multipolarities. The theoretical $\alpha_K^{theo}(E_i(XL))$ were received by square interpolation of the tabulated data [8] to the required energies with use of the computer code [9]. Having calculated the k, we used I_γ taken from Table 6 and I_K from [2] to calculate $\alpha_K^{exp}(E_i)$ and transition multipolarities, see Table 7 and Fig. 4. Multipolarities of some double (triple) transitions were also determined. To extract multipolarity information from the measured intensities, a special compilation was made based upon the measured gamma-ray intensities and theoretical K-shell conversion coefficients. The calculated K-electron internal conversion intensities for various multipolarity characters for the doublet (triplet) transitions are given in Table 8(9). The total K-ICE intensity for each doublet (triplet) was then compared to the measured I_K values. Sums that coincide with measured values within experimental uncertainties are underlined. As can be seen from Table 8(9) it was possible in such a way to assign more definite multipole characters to some transitions of those doublets (triplets).

For a number of transitions α_K^{exp} exceeded $\alpha_K^{theo}(M1)$, which can be explained by $E0$ or $E0 + M1$ multipolarities of those transitions. The transitions with $M2$ multipolarities were not observed due to their insignificant reduced probabilities $B(M2)$. The $M1$ multipolarities were assigned tentatively but those transitions might have an $E0$ or $M1+E2$ admixture as well. Establishing of such a multipolarity would require more sophisticated experiments, e.g. studies of the angular distribution of γ-quanta emitted from oriented nuclei. For most of the transitions,

the $E0$ admixtures were determined for the first time. Determination of $E0$ and $M1 + E0$ multipolarity is based on correct calculation of the intensity K-conversion electrons. For a number of K-conversion lines their intensities could turn out to be too high provided there exist overlaps of those lines with L-,M-, and N – conversion lines from other transitions. We calculated the maximum $I_L + I_M + I_N$ intensities (in accordance with possible multipolarities) for the transitions that were known before. They are enclosed in square brackets as we suppose that corrections for them had been made (see [1]). For the transitions which we observed for the first fime (I_γ is given with its uncertainity) as well as for the transitions that were not observed we determined only upper limits to their I_γ, see Table 10. On the basis of the Table 10, one can conclude that for the transitions with energies higher than 400 keV, such corrections for overlapping of $L + M + N$ conversion electrons belonging to new and possible transitions are negligible.

The $E0$ admixture is supposed to be proved if the following equation is satisfied :

$$\alpha_K^{exp} - 3\Delta\alpha_K^{exp} > \alpha_K^{theo}(M1)$$

We have found nine ($M1 + E0$) transitios obey the above equation. We surmise that transitions meeting a weaker condition :

$$\alpha_K^{exp} - 2\Delta\alpha_K^{exp} > \alpha_K^{theo}(M1) > \alpha_K^{exp} - 3\Delta\alpha_K^{exp}$$

still may have $M1+E0$ multipolarity, and enclose them in parentheses. We observed 19 such transitions, 8 of which are doublet ones.

We calculated the gamma-ray intensity upper limits for even those transitions where only K-conversion coefficients had been known, and than estimated their α_K^{exp} lower limits. Of these values 11 ones meet the stronger equation above, while 7 more — the weaker one. The multipolarities of these transitions may be either $E0$ or $M1 + E0$. As we have not observed tha gamma-rays corresponding to the decay of ^{152}Tb for these latter transitions, the inexactness in conclusion on their multipolarity becomes even greater.

The fundamental property of a $E0$ transition is its electron conversion probability $W_e(E0)$:

$$W_e(E0) = \rho^2(E0)\Omega_e$$

The ρ depends linearly on the matrix elements :

$$\rho(E0; i \to f) = \frac{\langle f|M(E0)|i\rangle}{eR^2},$$

containing the information on nuclear structure, Ω_e is the electronic factor, which depends on wave-function overlapping between the electron and the nucleus, nuclear charge Z and transition energy. It does not take into account nuclear structure [10, 11]. The main property of a monopole transition is its matrix element $\rho(E0)$. Its value can be extracted from the experimental data using the relation [12] :

$$\rho^2(E0; 0_i^+ \to 0_f^+) = \frac{I_K(E0; 0_i^+ \to 0_f^+)}{I_K(E2; 0_i^+ \to 2_j^+)} \frac{\alpha_K(E2; 0_i^+ \to 2_j^+)}{\Omega_K(E0; 0_i^+ \to 0_f^+)} W_\gamma(E2; 0_i^+ \to 2_j^+)$$

where $W_\gamma(E2; 0_i^+ \to 2_j^+)$ is the absolute $E2$ probability of a transition between a 0_i^+ level and a lower 2_j^+ one.

$$W_\gamma(E2; 0_i^+ \to 2_j^+) = \frac{\ln 2}{T_{1/2}(0_i^+)_{(lev)}} \times \frac{I_\gamma(E2; 0_i^+ \to 2_j^+)}{\sum_{m=1}^{i-1} I_{im}^{tot}},$$

where I_{im}^{tot} is the total intensity of transitions between level i and lower $m = i-1, i-2, ...1$ levels (1 marks the ground state). Unfortunately, lifetimes of only two excited states are known : 615 keV, 0^+, $T_{1/2}$ = 37(8) ps and 930 keV 2^+, $T_{1/2}$ = 7.3(6) ps [12], deexcited by $E0$ and $E0+M1+E2$ transitions, respectively. the $M1+E2$ mixing parameter δ = -3.05(14) for the 586 keV transition was determined from the $\gamma\gamma(\Theta)$ correlation measurements [13]. Using the data from Tables 6 and 7, $T_{1/2}$ and δ we calculated :

$$\rho^2(930, 2^+ \to 344, 2^+) = 46(4) \times 10^{-3}$$

$$\rho^2(615, 0^+ \to 0, 0^+) = 66(14) \times 10^{-3}.$$

The latter ρ^2 can be compared to the calculated one $\rho^2_{calc} = 79 \times 10^{-3}$, which refers to maximum mixture of spherical and deformed state wave-functions ($\beta_{def.} = 0.192$) [14]. It is interesting to compare the ratio of matrix elements of the transitions between the lowest 0^+ levels, which is $|\frac{\rho_{1047}}{\rho_{432}}| = 0.169$, to that of other nuclei. As for the

other $E0$ and $M1 + E0$ transitions, only their reduced probability ratios (Rasmussen parameters) could be determined because the data on their lifetimes were absent.

$$X = \frac{B(E0; 0_i^+ \to 0_j^+)}{B(E2; 0_i^+ \to 2_k^+)} \qquad \text{for transitions } 0^+ \to 0^+$$

or

$$X = \frac{B(E0; I_i \to I_f)}{B(E2; I_i \to I_k)} \qquad \text{for transitions } I_i = I_f \neq 0$$

One can calculate this parameter from the experimental data using the relation [15] :

$$X = 2.56 \times 10^{-6} A^{4/3} \frac{E_\gamma^5(E2) I_K(E0)}{\Omega_K(E0) I_K(E2)} \alpha_K(E2)$$

As a rule, the multipolarity mixtures $E0+M1+E2$ were not known quantitatively, therefore, the parameters X_1 and X_2 shown in Table 10 were supposed to have either $E0 + M1$ (with $\delta^2 = 0$) or $E0 + M1 + E2$ (with $\delta^2 = 1$) multipolarities. Multipolarity admixtures q were calculated as :

$$q^2 = \frac{(1+\delta^2)\alpha_K^{exp} - \alpha_K^{M1} - \delta^2 \alpha_K^{E2}}{\alpha_K^{E2}}; \qquad \delta^2 = \frac{I_\gamma^{E2}}{I_\gamma^{M1}}$$

X values versus level energies are given in Fig. 5. One can observe their monotonous growing, which proves qualitative changes in the structure of the states with their increasing excitation energy.

J.D. acknowledges support from GACR Grant No. 202/99/0149.

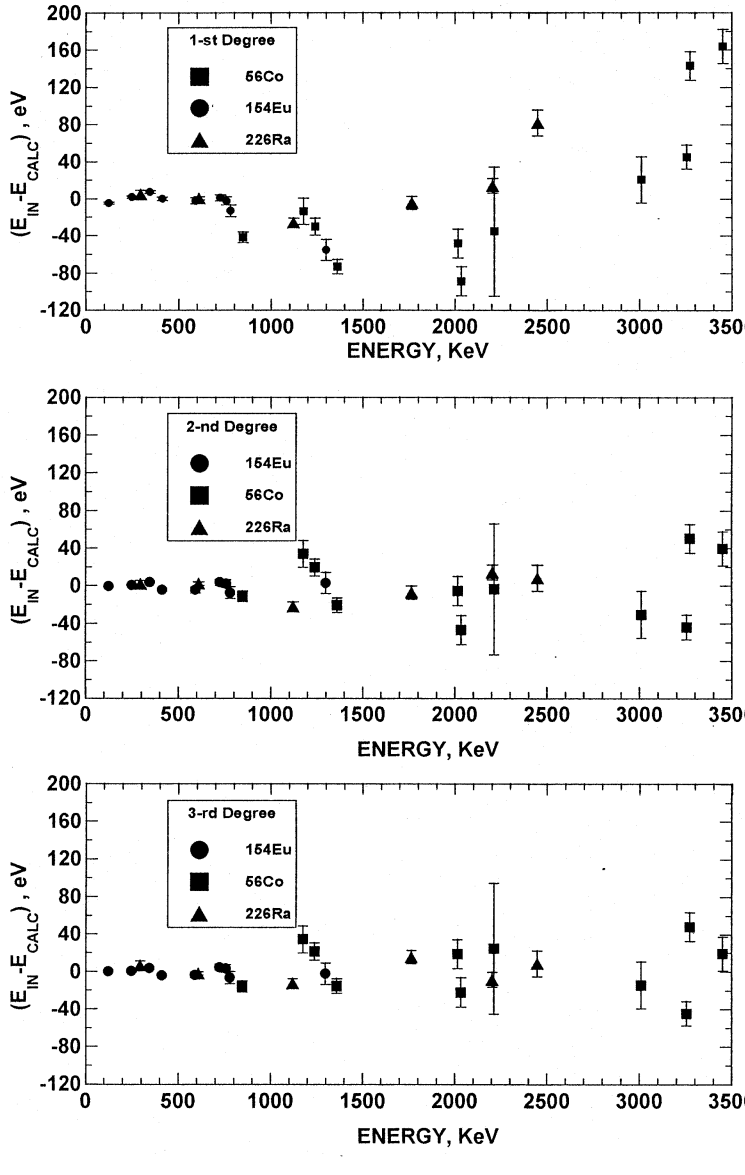

Figure 1. Experimental fitted energy residuals ($E_{in} - E_{calc}$).

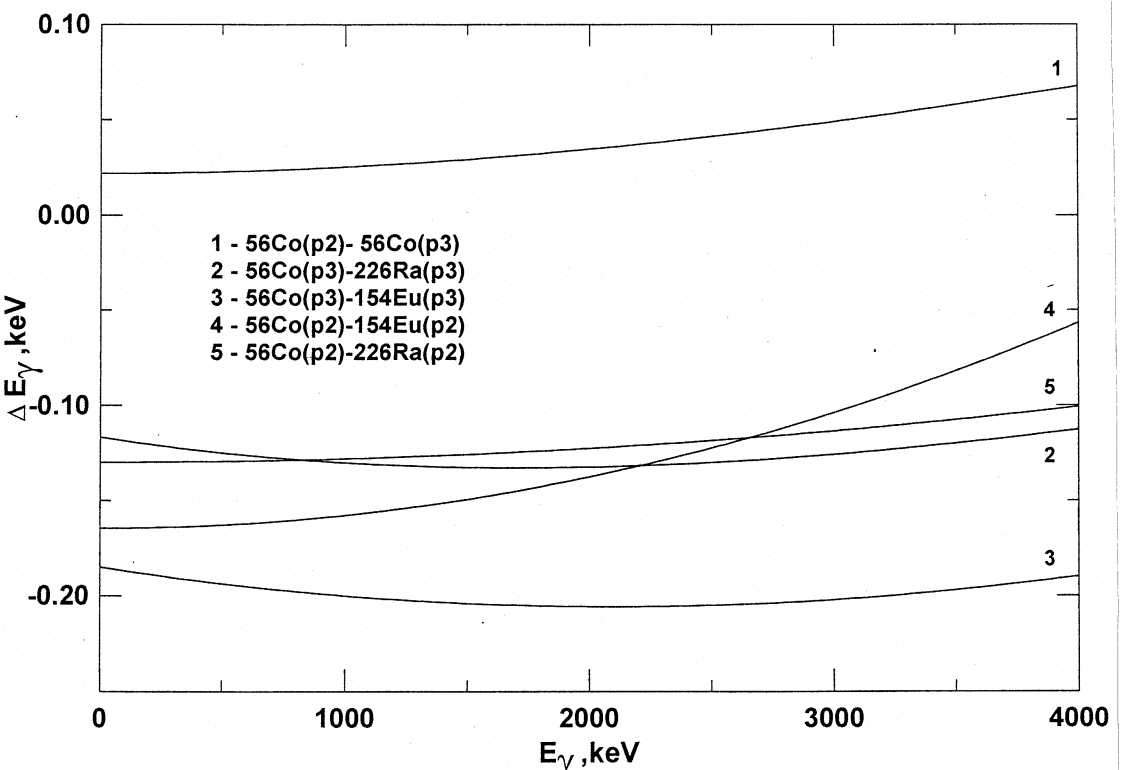

Figure 2. Difference of the non-linearity determined with standard isotopes ^{56}Co, ^{154}Eu and ^{226}Ra using 2nd and 3rd order polynomials.

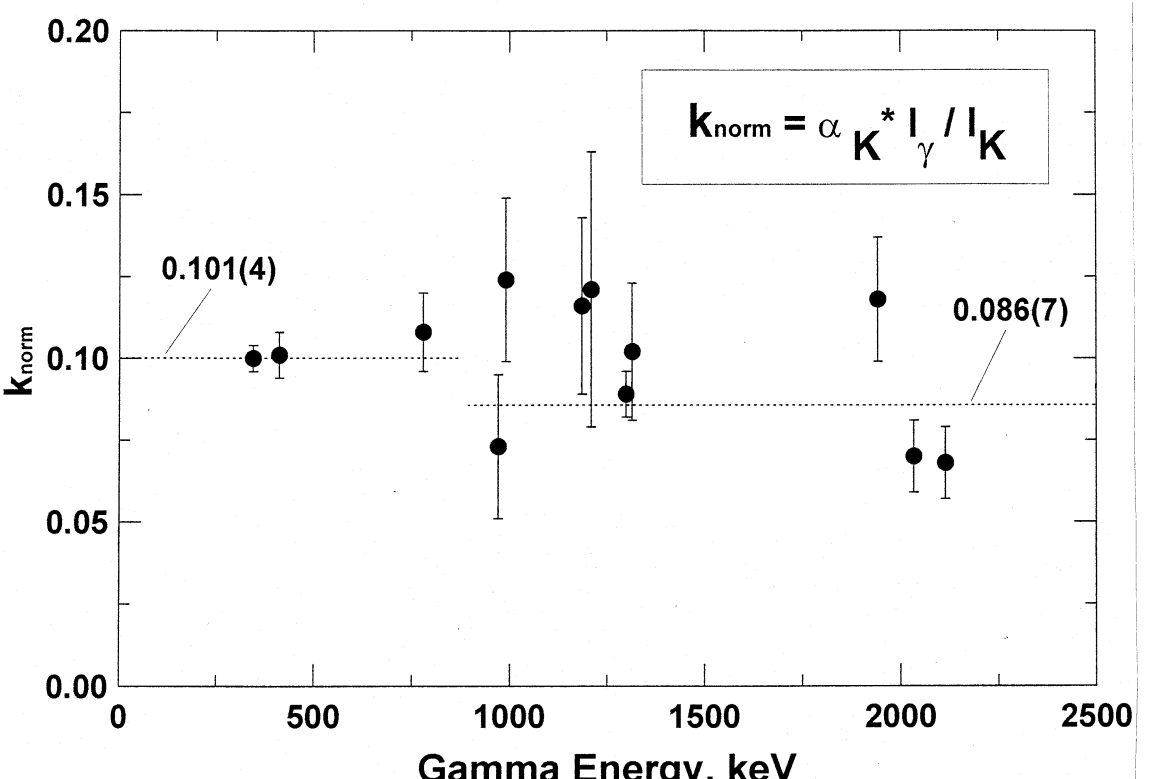

Figure 3. Calculation of the coefficient k connecting I_K and I_γ internal units.

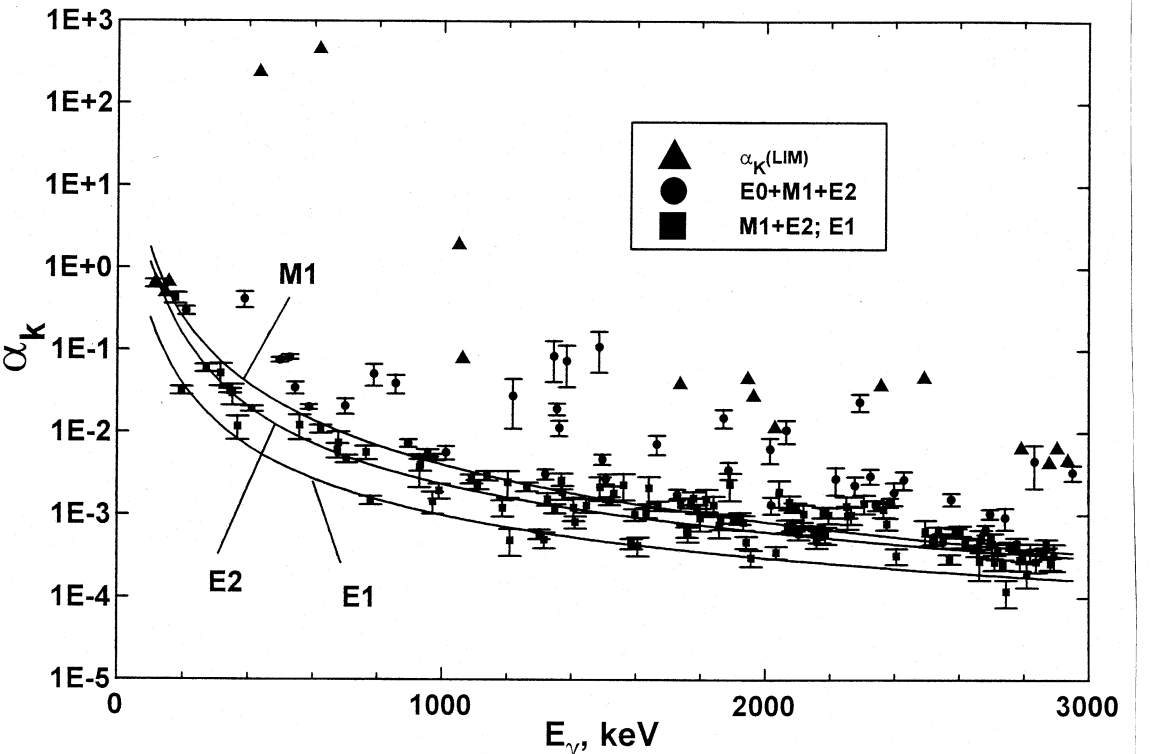

Figure 4. Comparison of $\alpha_K^{exp}(E_i)$ to $\alpha_K^{theo}(E_i, XL)$, $XL = M1, E1, E2$.

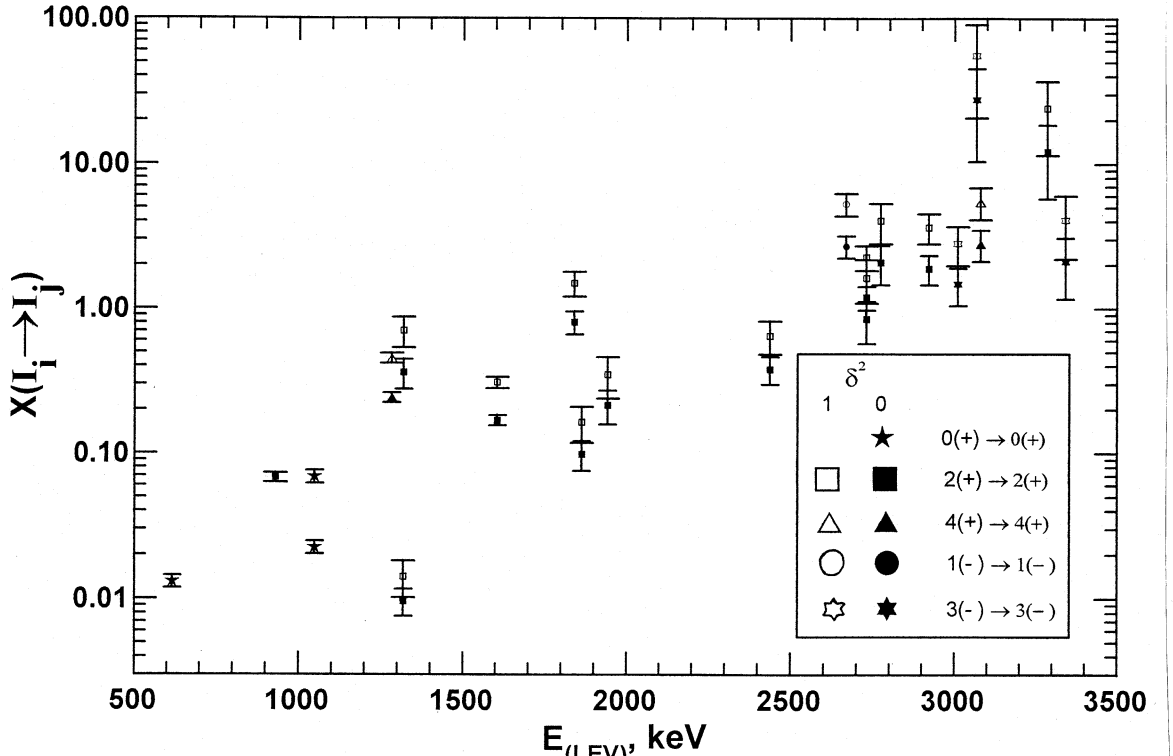

Figure 5. Dependence of the Rasmussen parameters (X) on energies of the initial levels that are deexcited by the given transitions.

Table 1. Example of channel-energy fit of peaks made with one and two gaussians

N, chan	ΔN, chan	FWHM, chan	E_γ, keV	$S_\gamma \times 10^{-3}$, counts	χ^2	E'_γ, keV	E_γ - E'_γ, keV	$\chi^{2'}$
1529.850	0.046	6.75	344.242	58015	10540	344.280	0.038(11)	223
1826.190	0.034	7.06	411.091	6251	299	411.122	0.031(9)	7
2602.580	0.038	7.74	586.232	23213	1990	586.265	0.033(8)	10
2764.550	0.036	7.78	622.770	2424	72	622.797	0.027(8)	2
2996.020	0.037	8.12	674.986	2033	34	675.013	0.037(11)	4
3121.600	0.029	8.40	703.316	6570	170	703.406	0.090(9)	1
3394.340	0.035	8.90	764.843	7425	364	764.881	0.038(9)	4
3456.390	0.038	8.38	778.841	14928	1110	778.892	0.051(10)	13
3963.810	0.032	8.55	893.310	1473	35	893.357	0.047(10)	1
4129.070	0.036	8.93	930.591	4582	39	930.562	0.029(11)	7
4393.060	0.027	8.98	990.146	1965	30	990.182	0.036(13)	5
4483.650	0.020	9.43	1010.582	1074	20	1010.623	0.041(15)	1
4920.720	0.020	9.12	1109.183	7509	76	1109.224	0.041(11)	4
5046.320	0.019	9.47	1137.518	2197	19	1137.577	0.059(12)	2
5595.000	0.026	10.46	1261.300	2291	22	1261.338	0.038(11)	2
5762.530	0.039	9.77	1299.094	4911	238	1299.178	0.084(12)	1
5881.070	0.033	10.32	1325.837	2000	41	1325.857	0.020(13)	1
5979.930	0.022	10.02	1348.140	1967	21	1348.201	0.061(15)	2
7035.260	0.034	10.67	1586.227	1949	40	1586.297	0.070(14)	1
7394.880	0.024	11.05	1667.360	1351	12	1667.432	0.063(17)	2
7793.910	0.036	11.82	1757.385	1305	24	1757.473	0.088(17)	1
8608.450	0.049	11.92	1941.155	1333	52	1941.234	0.079(18)	1
10487.500	0.093	12.73	2365.103	669	13	2365.173	0.070(26)	1
10532.460	0.050	12.91	2375.247	1314	54	2375.353	0.106(26)	1
10663.850	0.048	13.03	2404.892	2096	101	2405.009	0.117(26)	1
11246.270	0.047	13.32	2536.301	458	14	2536.405	0.104(33)	1

comment: $E_\gamma(E'_\gamma)$ are the transition energies determined from peaks fitted by one(two) gaussians, $\chi^2(\chi^{2'})$ – corresponding fit qualities.

Table 2. Parameters of energy fit to Standard Radioactive Sources

	^{56}Co+Tb	^{154}Eu+Tb	^{226}Ra+Tb
E_γ(min)	344.279	123.071	295.207
E_γ(max)	3451.119	1299.140	2447.709
n	15	9	10
χ^2(1st)	33.0	6.5	2.6
χ^2(2nd)	5.0	1.9	2.5
χ^2(3rd)	4.5	2.2	1.3

Table 3. Reference lines from internal calibration

Adopted value	Tb152+Eu152	Tb152+Eu154	Tb152+Ra226	Tb152+Co56
$E_\gamma(\Delta E_\gamma)$	$E_\gamma(\Delta E_\gamma)$	$E_\gamma(\Delta E_\gamma)$	$E_\gamma(\Delta E_\gamma)$	$E_\gamma(\Delta E_\gamma)$
195.17(7)	195.19(7)	195.15(7)		
271.09(7)	271.06(7)	271.11(7)		
315.16(7)	315.17(7)	315.17(7)	315.14(7)	
344.2785(13)*	344.27(7)	344.27(7)	344.28(7)	344.28(7)
411.1165(13)*	411.12(7)	411.12(7)	411.12(7)	411.12(7)
586.27(7)	586.28(7)	586.28(7)	586.25(7)	586.26(7)
622.79(7)	622.80(7)	622.80(7)	622.78(7)	622.78(7)
764.89(7)	764.89(7)	764.90(7)	764.88(7)	764.88(7)
778.9045(24)*	778.90(7)	778.91(7)	778.90(7)	778.90(7)
1089.737(5)*	1089.73(7)	1089.73(7)	1089.75(7)	1089.75(7)
1299.140(9)*	1299.14(7)	1299.14(7)	1299.18(7)	1299.13(7)
1325.86(7)	1325.82(7)	1325.89(7)	1325.85(7)	1325.87(7)
1517.78(7)	1517.69(7)	1517.77(7)	1517.86(7)	1517.79(7)
1586.22(7)	1586.17(7)	1586.21(7)	1586.23(7)	1586.26(7)
1667.38(8)			1667.36(7)	1667.40(8)
1757.42(7)			1757.39(7)	1757.46(7)
1789.20(8)			1789.19(8)	1789.22(8)
1902.45(8)			1902.43(8)	1902.48(8)
2185.24(9)			2185.18(9)	2185.29(9)
2536.30(7)				2536.30(7)
2719.61(8)				2719.61(8)
2940.15(11)				2940.15(11)
3324.22(11)				3324.22(11)
3479.14(14)				3479.14(14)

Note. * – The energy of the peak is taken from ref. [4]

Table 4. Number of ballast peaks (BP) in the region $900 < E_\gamma < 4000$ keV

Type of BP	All	$S_\gamma(BP(E_\gamma)) > 0.2S_\gamma^{(lim)}(E_\gamma)$	$S_\gamma(BP(E_\gamma)) > S_\gamma^{(lim)}(E_\gamma)$
Background	32	9	9
Sumpeaks	248	100	74
SEP	504	319	133
DEP	504	261	75

Table 5. Number of peaks whose intensities were reduced by substracting the corresponding BP intensities

c$\equiv S_\gamma(BP(E_\gamma))/S_\gamma(E_\gamma)$ %								
c<1	1≤c≤5	5<c≤10	10<c≤20	20<c≤30	30≤c≤40	40<c≤50	50<c≤70	70<c<100
13	107	51	55	39	20	18	20	8

Table 6. Energies and intensities of γ-transitions from the ^{152}Tb$\longrightarrow$ ^{152}Gd decay

$E_\gamma(\Delta E_\gamma)$	$I_\gamma(\Delta I_\gamma)$	Comment	$E_\gamma(\Delta E_\gamma)$	$I_\gamma(\Delta I_\gamma)$	Comment
115.3	<0.6	b	1622.4(4)	1.48(28)	n
117.25(7)	7.85(22)	p	1626.39(19)	2.14(18)	n,p
143.8	<0.5	b	1631.42(8)	36.1(8)	d,c,p
155.1	<0.4	b	1634.0(3)	1.08(25)	n,c,p
159.16(16)	1.47(16)	n,p	1640.08(9)	6.84(22)	c,p
160.77(9)	2.52(15)	n	1645.92(8)	10.50(26)	c,p
169.50(12)	3.20(29)	n	1663.67(14)	6.7(4)	c,p
175.14(9)	3.8(4)	n,c,p	1667.38(8)	103.4(24)	c,p
178.58(11)	1.89(16)	n,p	1681.53(8)	6.57(17)	c,p
181.3(3)	1.03(23)	n	1685.28(16)	1.63(12)	n
185.17(16)	1.23(28)	n	1687.69(11)	2.11(13)	n
195.17(7)	62.4(14)	c,p	1690.68(9)	3.06(13)	n,p
196.34(17)	4.7(5)	n	1694.60(13)	2.64(12)	n,p
209.14(8)	5.68(21)	c,p	1711.02(9)	3.36(11)	n,c,p
218.42(9)	2.18(11)	n,p	1714.65(25)	0.66(9)	n,p
248.75(9)	9.9(12)	c,p	1727.72(8)	11.59(26)	c,p

271.09(7)	1499(33)	c,p	1732.42(11)	1.82(16)	n,p
296.31(21)	1.05(21)	n	1735.8	<0.3	b
298.06(21)	1.08(16)	n,p	1737.03(9)	6.55(17)	n,c,p
301.82(26)	0.78(22)	n,p	1739.46(8)	12.14(27)	c,p
315.16(7)	127.9(28)	c,p	1748.34(14)	0.68(7)	n
322.18(13)	1.37(14)	n	1757.42(7)	101.6(23)	c,p
324.90(7)	6.62(30)	n,c,p	1761.22(16)	8.9(5)	c,p
334.02(11)	3.74(21)	n	1771.43(8)	51.8(11)	c,p
335.56(7)	9.33(26)	n,c,p	1776.3(3)	2.3(3)	n,p
344.2785(13)	10000(250)	a,c,p	1778.78(9)	16.5(5)	c,p
351.73(7)	36.6(9)	c,p	1785.15(11)	7.7(4)	n,c,p
353.78(9)	4.48(20)	n,c,p	1789.20(8)	89.9(17)	d,c,p
362.33(9)	3.09(14)	n	1792.71(14)	8.0(6)	n,c,p
364.84(16)	1.42(17)	n	1796.83(14)	8.3(5)	n,c,p
366.15(9)	4.70(26)	n,c,p	1798.45(9)	15.8(6)	c,p
367.80(7)	55.0(14)	c,p	1802.67(9)	10.24(27)	c,p
368.66(21)	4.2(10)	n	1809.53(10)	12.7(4)	c,p
381.7(3)	0.88(22)	n	1811.33(28)	2.5(3)	n,p
385.5(3)	1.9(6)	n	1818.56(9)	9.26(28)	c,p
387.80(7)	58.6(20)	c,p	1825.37(9)	23.8(5)	c,p
390.82(15)	1.17(19)	n,c,p	1841.15(9)	12.3(3)	d,c,p
407.12(21)	2.16(27)	n,c,p	1844.83(12)	2.27(11)	n
411.1165(13)	567(14)	a,c,p	1857.48(8)	27.2(6)	c,p
421.40(18)	1.22(12)	n	1861.94(8)	72.0(15)	c,p
427.85(11)	3.15(21)	n,c,p	1870.55(18)	1.19(16)	n
432.5	<0.3	b,p	1875.35(12)	2.38(18)	n
441.02(8)	7.15(19)	c,p	1886.08(13)	4.6(3)	c,p
453.26(24)	0.88(20)	n	1891.45(17)	6.2(3)	
454.82(28)	0.79(18)	n,p	1896.52(21)	5.3(4)	n
456.92(7)	6.49(27)	c,p	1902.45(8)	268(5)	d,c,p
460.29(22)	0.96(21)	n	1907.51(18)	4.1(3)	
465.68(10)	4.27(14)		1914.71(13)	8.0(3)	
471.98(9)	3.38(14)	c,p	1917.55(15)	5.14(13)	n,c,p
482.34(9)	9.14(23)	c,p	1921.00(8)	66.1(14)	c,p
489.59(13)	3.8(3)	n,c,p	1932.94(12)	5.71(28)	c,p
490.66(9)	9.2(3)	c,p	1941.23(8)	110.8(23)	c,p
491.84(27)	1.5(3)	n	1944.8	<0.3	b,p
493.81(7)	22.3(6)	c,p	1951.17(19)	3.90(27)	n
496.37(7)	23.0(5)	c,p	1955.36(8)	54.8(12)	c,p
500.23(12)	1.02(16)	n,p	1962.9	<0.3	b
503.43(7)	10.16(27)	c,p	1965.42(19)	2.41(14)	n,p
520.30(8)	9.7(4)	c,p	1967.9(5)	0.89(13)	n
522.03(18)	1.46(19)	n	1970.49(9)	7.81(21)	c,p
526.85(9)	41.4(9)	c,p	1975.65(8)	11.83(26)	c,p
534.21(9)	8.25(20)	c,p	1979.93(19)	0.72(12)	
543.58(7)	30.3(7)	c,p	1983.41(8)	11.42(27)	c,p
547.47(7)	11.14(29)	c,p	1986.8(4)	0.75(15)	n,p
554.24(21)	1.71(16)	n	1993.87(8)	14.4(3)	c,p
557.67(7)	17.5(5)	d,c,p	2004.93(17)	1.09(9)	n,p
562.98(9)	10.53(28)	c,p	2014.48(20)	1.18(23)	n
569.04(20)	1.22(16)	n	2018.09(14)	3.00(12)	
571.54(10)	2.48(15)	n	2020.67(14)	1.90(11)	n,p

575.40(14)	1.29(13)	n	2029.5	<0.3	
577.57(9)	2.74(14)	n,c,p	2033.89(9)	21.6(5)	c,p
579.63(9)	4.70(24)	n,c,p	2043.65(10)	15.6(4)	t,c,p
583.00(11)	4.5(4)	n,p	2051.26(11)	4.06(14)	
586.27(7)	1454(30)	c,p	2058.47(9)	1.48(13)	n,c,p
595.83(11)	2.43(29)	n	2064.90(16)	1.24(16)	n,c,p
597.57(11)	1.68(11)	n,p	2069.00(8)	14.5(3)	c,p
603.18(14)	1.75(12)	n,c,p	2073.51(17)	1.79(21)	n
615.6	<0.4	b,p	2076.21(10)	5.93(23)	c,p
622.79(7)	145(3)	c,p	2078.63(9)	5.21(24)	c,p
633.60(9)	2.93(11)	p	2082.22(18)	1.99(12)	n
638.35(10)	1.71(22)	n,p	2086.20(10)	4.47(15)	
641.20(7)	9.32(22)	c,p	2093.51(8)	33.3(7)	d,c,p
645.83(14)	1.41(14)	n	2103.54(9)	10.11(26)	d,c,p
648.31(7)	16.6(4)	c,p	2113.70(9)	13.6(3)	c,p
651.06(19)	1.27(12)	n	2118.66(9)	8.74(23)	c,p
656.42(9)	5.37(24)	p	2127.99(11)	5.30(21)	
658.83(11)	4.18(28)	c,p	2140.35(16)	2.60(14)	n
662.02(10)	2.56(28)	n,p	2150.85(8)	35.2(7)	c,p
667.46(13)	2.18(13)	n	2158.72(10)	11.0(3)	c,p
675.01(7)	83.5(17)	c,p	2162.05(15)	5.11(24)	n,c,p
678.61(7)	35.3(8)	c,p	2169.16(9)	14.6(3)	d,c,p
681.3(3)	1.7(6)	n	2172.45(11)	4.94(17)	n,c,p
684.12(9)	2.7(3)	n,p	2176.44(11)	5.75(18)	
687.62(14)	1.5(4)	n,p	2179.42(11)	9.30(25)	c,p
693.13(16)	4.19(28)	c,p	2182.10(15)	3.94(19)	n,c,p
697.20(16)	2.4(8)	n,c,p	2185.24(9)	35.8(7)	c,p
699.25(10)	12.6(9)	c,p	2192.22(10)	1.57(11)	n
703.39(7)	371(7)	d,c,p	2196.20(9)	14.7(3)	c,p
708.98(8)	5.76(21)	c,p	2201.65(26)	1.99(20)	n,p
712.82(8)	17.7(6)	c,p	2209.71(13)	5.02(29)	n,p
715.19(8)	7.94(20)	c,p	2217.40(9)	7.49(19)	n,c,p
722.00(12)	2.00(14)	n,c,p	2220.81(21)	2.37(14)	n
723.67(10)	3.22(13)	n,p	2223.71(19)	1.41(19)	n
730.95(11)	4.7(9)		2226.01(23)	2.71(18)	n,c,p
738.69(9)	33.6(9)	c,p	2235.76(14)	3.37(12)	n
747.29(14)	1.57(11)	n,c,p	2239.13(24)	1.18(13)	n
750.06(9)	1.97(20)	n,c,p	2251.41(9)	12.61(28)	c,p
752.59(9)	5.0(4)	n,c,p	2254.54(9)	15.0(3)	c,p
758.01(11)	3.61(24)	n	2257.22(22)	2.36(15)	n,c,p
758.8(4)	2.8(6)	n	2260.05(11)	10.43(25)	c,p
764.89(7)	432(10)	c,p	2262.9(4)	1.58(18)	n
778.9045(24)	872(18)	a,c,p	2265.33(9)	13.2(3)	c,p
787.18(12)	3.33(15)	n	2269.68(25)	0.99(17)	n
788.88(10)	4.53(18)	n,p	2275.07(19)	2.68(22)	n
792.56(11)	3.15(20)	n,c,p	2276.87(17)	2.57(25)	n
794.73(7)	27.4(7)	c,p	2281.44(11)	2.52(10)	n
805.84(9)	3.24(14)	n,p	2287.66(27)	0.49(10)	n
810.44(23)	1.55(18)	n,p	2291.46(19)	1.24(12)	n
812.80(8)	31.4(8)	c,p	2306.15(10)	4.22(13)	c,p
814.38(16)	5.5(5)	n,d,c,p	2312.00(10)	4.87(14)	n,c,p
818.25(8)	16.0(4)	d,c,p	2317.61(24)	1.03(10)	n,c,p

824.70(13)	1.69(11)	n	2322.3(4)	1.40(29)	n
829.57(26)	1.29(34)	n	2324.32(17)	5.46(29)	c,p
831.94(8)	17.9(5)	c,p	2335.00(16)	1.42(8)	n,p
834.73(18)	3.65(17)	n	2342.57(9)	20.3(4)	c,p
837.08(11)	3.23(17)	n,p	2347.53(11)	4.38(16)	
839.6(4)	2.1(4)	n,c,p	2350.30(15)	2.30(14)	n,c,p
841.10(9)	7.2(4)	c,p	2354.19(14)	2.61(16)	n
847.62(24)	1.40(20)	n	2357.0	<0.3	b
850.49(28)	4.7(4)	n,c,p	2365.13(9)	57.0(14)	c,p
852.1(5)	3.8(8)	n	2375.34(9)	122.5(26)	c,p
855.00(9)	10.3(12)	t,c,p	2382.27(16)	2.15(14)	n
857.33(11)	12.6(9)	c,p	2384.94(9)	14.5(3)	c,p
860.84(14)	1.63(16)	n,p	2388.72(11)	3.80(12)	n,c,p
865.62(8)	6.03(24)	n,c,p	2398.53(26)	8.6(10)	
868.94(11)	4.13(15)	n,p	2405.00(9)	207(4)	c,p
874.85(26)	0.67(20)	n,p	2411.45(18)	0.81(9)	n
878.13(19)	3.8(3)	n,c,p	2420.43(20)	0.87(9)	n
880.29(10)	6.49(21)	n,p	2428.36(11)	9.27(25)	
883.30(11)	2.11(20)	n	2437.11(21)	1.32(10)	n,p
887.32(10)	5.15(19)	n,p	2440.3(4)	0.50(9)	n
893.34(7)	100.9(21)	c,p	2444.39(22)	0.95(11)	n
902.46(8)	22.5(6)	c,p	2450.24(15)	0.80(7)	n
909.15(7)	19.5(6)	c,p	2462.73(21)	0.77(8)	n
911.73(13)	1.95(11)	n	2469.72(14)	1.45(9)	n
914.35(7)	8.19(24)	p,c	2472.44(15)	1.78(9)	n
919.20(9)	1.77(12)	n	2479.26(22)	1.62(11)	
923.98(15)	1.72(18)	n	2481.75(29)	0.76(11)	n,p
928.43(7)	56.8(12)	c,p	2488.97(12)	3.89(16)	n
930.58(7)	231(8)	c,p	2491.4	<0.3	b
932.09(8)	30.5(11)	c,p	2495.53(9)	13.8(3)	c,p
937.04(9)	25.6(10)	c,p	2503.96(22)	0.83(10)	n
939.84(9)	5.30(18)	n,c,p	2507.8(4)	0.45(10)	n
945.26(13)	2.25(19)	n	2513.9(4)	0.71(18)	n,p
947.08(28)	0.99(18)	n,p	2518.42(9)	17.9(4)	c,p
950.34(16)	2.27(10)	n,p	2523.92(9)	13.1(3)	p
953.07(9)	9.57(24)	d,c,p	2536.30(7)	39.5(11)	c,p
970.32(7)	118.9(25)	c,p	2544.58(18)	0.74(9)	n
974.05(9)	472(10)	c,p	2548.10(25)	0.88(8)	n
979.04(12)	4.16(24)	n,p	2551.48(11)	4.82(12)	
981.18(24)	1.1(4)	n	2555.34(18)	1.92(10)	n
984.90(8)	9.3(5)	c,p	2557.91(12)	3.89(12)	p
990.19(7)	112.4(23)	c,p	2569.85(10)	25.3(6)	p
993.14(11)	9.9(4)	n,c,p	2572.6(4)	2.31(22)	n
998.37(11)	2.05(11)	n,p	2575.82(17)	4.46(19)	p
1000.41(20)	1.22(12)	n,p	2579.82(17)	5.27(22)	
1004.2(3)	0.99(15)	n,p	2583.0(4)	4.7(8)	p
1010.60(7)	63.2(13)	c,p	2584.89(27)	8.7(8)	p
1016.60(9)	11.2(3)	c,p	2588.36(8)	57.1(12)	p
1022.73(11)	2.01(13)	n,p	2597.04(16)	1.92(10)	n
1027.16(21)	1.67(19)	n,c,p	2600.69(18)	4.46(23)	
1030.71(11)	3.1(4)	n	2602.85(11)	10.0(3)	
1036.74(7)	17.2(4)	c,p	2619.61(9)	41.2(9)	

1040.6(3)	1.00(21)	n	2629.74(13)	0.79(6)	n
1045.31(23)	1.13(15)	n,p	2636.93(10)	4.25(10)	p
1047.9	<1.3	b,p	2644.74(16)	2.71(17)	n,p
1052.15(7)	18.5(4)	c,p	2655.29(10)	8.72(25)	p
1056.79(9)	3.56(13)	n,c,p	2662.55(10)	26.9(5)	p
1061.6	<1.6	b	2665.18(12)	10.69(28)	n
1066.23(26)	1.71(13)	n,p	2668.13(10)	20.5(4)	
1069.15(9)	9.5(3)		2678.03(17)	1.75(11)	n
1072.16(15)	3.1(4)	n,c,p	2680.88(11)	6.02(16)	
1075.87(9)	4.9(6)	n,c,p	2687.39(12)	2.60(8)	
1083.96(10)	12.2(5)	n,d,c,p	2694.48(11)	7.84(23)	
1085.68(11)	21.5(7)	t,c,p	2697.99(10)	28.0(6)	p
1087.12(10)	20.7(8)	c,p	2702.98(10)	9.93(24)	
1089.737(5)	141.5(29)	a,c,p	2709.47(9)	27.4(6)	p
1092.26(14)	5.4(3)	n,c,p	2719.61(8)	40.1(9)9	p
1096.60(19)	3.1(3)	n,p	2722.45(15)	9.5(4)	n
1098.30(27)	1.8(3)	n	2729.25(11)	2.61(9)	n
1106.59(8)	60.6(18)	c,p	2734.06(10)	14.2(3)	p
1109.20(7)	401(9)	c,p	2740.93(12)	3.92(12)	
1117.15(11)	3.69(14)	n,c,p	2744.10(10)	12.18(26)	p
1119.42(17)	1.65(15)	n	2754.70(10)	15.5(3)	p
1128.65(10)	4.3(5)	n	2761.15(12)	1.74(7)	p
1130.98(7)	22.3(5)		2768.27(10)	4.13(10)	p
1137.56(7)	134.9(29)	c,p	2772.44(18)	0.80(50	n,p
1141.68(10)	5.23(24)	n,c,p	2776.04(27)	1.28(11)	n
1144.94(16)	2.38(20)	n	2778.28(12)	3.95(12)	
1148.99(10)	6.7(3)	c,p	2787.86(11)	3.56(9)	
1155.48(13)	3.3(4)	n,p	2793.27(14)	3.08(11)	n
1157.18(16)	2.4(4)	n	2795.92(11)	10.40(23)	p
1159.82(7)	41.1(10)	c,p	2799.81(14)	1.78(7)	p
1164.17(9)	3.73(19)	n	2808.61(10)	6.96(16)	
1167.0(3)	1.9(4)	n,p	2816.84(15)	1.60(6)	
1171.19(27)	5.9(11)	p	2820.43(12)	3.28(9)	
1173.4(6)	1.4(3)	n	2824.17(27)	0.68(6)	n
1176.53(9)	4.32(17)	n,p	2833.50(12)	1.84(5)	
1185.73(7)	33.7(8)	c,p	2838.15(11)	3.72(8)	
1188.37(11)	5.62(23)	n,c,p	2845.25(12)	1.43(5)	n
1190.44(7)	60.4(12)	c,p	2859.06(13)	3.25(10)	n
1193.20(21)	2.3(3)	n	2861.75(11)	6.50(15)	
1198.97(11)	3.6(3)	n,p	2869.24(11)	7.51(16)	
1202.64(9)	8.95(29)	d,c,p	2873.2(4)	0.40(6)	n
1205.83(11)	17.6(7)	c,p	2882.39(11)	11.47(25)	
1209.03(9)	45.3(10)	c,p	2887.52(13)	2.43(8)	n,p
1215.20(11)	1.66(18)	n,p	2890.21(12)	4.75(11)	
1218.64(11)	3.47(13)	n	2893.15(11)	5.99(13)	
1221.95(12)	3.32(22)	n,c,p	2906.48(15)	7.22(23)	
1225.86(10)	2.20(18)	n	2910.0(6)	0.38(6)	n
1235.57(10)	7.25(25)	c,p	2914.42(14)	1.21(6)	p
1237.20(11)	3.46(27)	n	2918.46(21)	1.08(5)	n
1239.51(11)	3.37(21)	n	2921.85(14)	2.12(7)	
1247.07(7)	20.9(6)	c,p	2927.29(11)	5.57(13)	
1250.7(4)	1.13(28)	n	2940.15(11)	11.40(24)	p

1253.48(9)	3.44(18)	n,c,p	2945.9(4)	0.33(5)	n
1258.45(10)	7.50(29)	n,p	2950.50(27)	0.49(6)	n
1261.32(8)	142(3)	c,p	2961.00(12)	2.61(7)	
1263.84(11)	11.0(4)	n,c,p	2971.46(14)	1.23(5)	
1275.04(7)	15.5(4)	c,p	2980.07(11)	4.78(10)	
1278.33(9)	4.1(6)	n	2983.78(11)	2.75(7)	
1284.42(9)	12.7(3)	c,p	2993.14(15)	2.82(8)	n
1289.64(9)	4.74(15)	c,p	2996.26(12)	4.32(10)	p
1299.140(9)	325(7)	a,c,p	2999.69(16)	4.99(8)	p
1308.07(16)	1.50(14)	n	3006.63(14)	1.18(4)	n,p
1314.66(9)	222(5)	d,c,p	3014.77(13)	2.20(5)	
1316.32(12)	31.0(24)	c,p	3018.13(15)	1.11(4)	n
1318.24(13)	42.0(17)	c,p	3022.50(14)	2.20(8)	
1325.86(7)	123.9(26)	c,p	3024.93(17)	1.24(6)	n
1336.54(8)	19.6(4)	c,p	3037.62(22)	0.87(5)	n
1338.5(4)	1.93(26)	n,p	3042.64(12)	10.99(23)	
1348.15(9)	134.3(27)	c,p	3056.19(12)	3.15(8)	
1352.98(11)	4.6(5)	n,c,p	3059.53(20)	0.95(5)	n
1360.43(11)	4.63(21)	c,p	3068.25(15)	1.27(5)	
1363.39(14)	4.11(25)	n,p	3085.05(15)	1.48(5)	
1365.69(8)	13.6(3)	c,p	3088.60(17)	0.91(4)	
1369.04(9)	20.0(5)	c,p	3094.73(12)	2.10(6)	
1372.04(9)	7.73(23)	c,p	3105.45(16)	1.72(7)	n,p
1375.76(21)	0.92(21)	n	3107.88(14)	2.52(8)	
1393.86(9)	7.26(19)	n,c,p	3112.27(27)	0.404(27)	n,p
1400.60(7)	24.4(5)	d,c,p	3115.6(3)	0.286(25)	n
1406.16(8)	16.0(4)	c,p	3122.25(18)	0.427(29)	n
1410.29(13)	11.6(16)	c,p	3132.3(4)	0.41(4)	n
1411.48(9)	101(3)	d,c,p	3135.00(28)	0.69(5)	
1414.40(14)	5.91(21)	n,c,p	3140.20(12)	2.88(7)	p
1417.18(15)	3.13(16)	n,c,p	3147.2(6)	0.18(3)	n
1420.76(8)	8.63(24)	c,p	3154.42(14)	1.86(5)	
1424.76(19)	1.92(18)	n,p	3158.87(12)	5.26(12)	
1427.32(7)	16.5(4)	c,p	3162.3(4)	1.8(2)	
1430.76(7)	14.8(6)	c,p	3164.54(18)	7.60(23)	
1434.54(11)	4.51(22)	n,c,p	3166.90(21)	2.02(17)	n
1436.67(9)	6.65(19)	p	3174.02(12)	3.16(8)	
1441.91(8)	18.2(5)	c,p	3180.51(22)	0.309(25)	n
1446.43(7)	38.7(8)	d,c,p	3190.1(3)	2.42(18)	
1449.45(31)	1.84(21)	n	3194.51(28)	0.47(3)	n
1454.08(12)	3.54(20)	n,c,p	3205.60(21)	4.83(11)	
1457.25(11)	2.90(22)	n,p	3211.74(29)	0.50(4)	n
1465.85(18)	0.68(22)	n	3223.80(17)	3.81(16)	
1471.45(15)	2.4(4)	n	3228.75(13)	2.09(5)	
1475.04(14)	1.5(5)	n,p	3232.48(16)	0.855(29)	n
1481.18(8)	9.8(5)	p,c	3236.76(18)	0.500(25)	n
1485.72(32)	2.79(25)	n	3244.90(22)	0.361(26)	
1489.60(10)	10.3(3)	c,p	3251.04(17)	0.602(27)	
1491.62(22)	2.66(19)	n,c,p	3261.0(5)	0.129(27)	n
1495.44(8)	16.3(6)	c,p	3265.88(22)	0.70(4)	n
1502.62(10)	2.40(8)	n,c,p	3268.70(16)	1.62(5)	
1506.90(8)	7.80(29)	c,p	3272.34(21)	0.734(29)	n

1514.61(14)	1.6(3)	n	3276.00(19)	1.20(3)	
1517.78(7)	102.5(21)	t,c,p	3284.24(15)	0.896(29)	
1521.57(16)	2.9(3)	n,c,p	3309.75(14)	1.54(4)	
1530.07(15)	1.55(13)	n,p	3324.22(11)	5.10(12)	
1532.75(10)	5.67(18)		3328.24(15)	1.34(4)	
1535.84(16)	2.06(17)	n	3338.12(16)	0.593(22)	
1544.29(8)	9.46(23)	c,p	3359.86(25)	0.192(14)	n
1547.95(9)	6.46(18)	n,c,p	3366.46(15)	0.735(24)	
1554.04(16)	2.13(19)	n,p	3380.23(15)	0.774(24)	
1558.07(12)	2.15(17)	n	3391.1(4)	0.127(14)	n
1562.45(8)	12.9(3)	c,p	3401.45(20)	0.297(16)	n
1565.97(8)	15.94(4)	c,p	3406.89(23)	0.233(14)	n
1571.25(8)	24.9(5)	c,p	3411.90(15)	0.842(24)	
1575.30(9)	9.40(25)	c,p	3459.70(29)	0.133(12)	n
1586.22(7)	145(3)	c,p	3479.14(14)	1.90(5)	
1593.37(9)	14.5(4)	n,c,p	3493.32(18)	0.359(14)	n
1596.75(7)	72.1(15)	d,c,p	3508.7(3)	0.131(12)	n
1598.90(8)	34.6(8)	c,p	3534.74(24)	0.187(12)	n
1605.72(7)	58.5(11)	d,c,p	3565.85(24)	0.152(10)	n
1610.11(19)	2.48(21)	n,p	3572.44(18)	0.388(14)	
1613.53(9)	8.25(28)	n,p	3595.29(27)	0.158(12)	n
1620.35(20)	4.11(27)	n	3621.7(4)	0.093(11)	n

Notes. a) Energy of this peak is taken from [4]. b) Energy of this transition is taken from ICE measurements. n) New transition. d) Double transition, see table 7 [16]. t) Triple transition, see table 7 [16]. c,p) Transition is placed in the decay scheme on the basis of gamma-gamma coincidencies. p) Transition is placed in the decay scheme on the basis of the balance of energies

Table 7: Multipolarities of transitions from ^{152}Tb$\longrightarrow$ ^{152}Gd decay

E_γ	$\alpha_K(\Delta_{\alpha_K})$	XL	E_γ	$\alpha_K(\Delta_{\alpha_K})$	XL
113.5	>0.64(17)	$\geq$E2	1891.45	2.4(10)E-3	(E2M1)
115.3	>0.71(17)	$\geq$E2	1902.46	9.2(17)E-4	M1
117.25	6.4(10)E-1	E2	1907.51	3.6(16)E-3	(M1)
143.8	>0.52(16)	M1	1921.00	9.2(21)E-4	M1(E2)
155.1	>0.71(20)	M1	1932.94	8.3(22)E-4	M1(E2)
175.14	4.3(9)E-1	M1	1941.23	4.7(11)E-4	E1
178.58	1.8(11)	E2,M1	1944.8	>4.9(17)E-2	(E0(M1))
195.17	d	E1	1955.36	3.1(9)E-4	E1
196.34	d	E1	1962.9	>3.0(12)E-2	(E0(M1))
209.14	3.0(5)E-1	(E0)M1	2014.48	6.4(26)E-3	(E0)M1
271.09	6.0(9)E-2	E2	2018.09	d	M1;E2
315.16	5.2(18)E-2	E2(M1)	2020.67	d	E2;M1
344.278	3.13(30)E-2	E2	2029.5	>1.2(5)E-2	(E0(M1))
351.73	3.0(10)E-2	E2	2033.89	3.6(9)E-4	E1

367.80	1.2(4)E-2	E1	2043.65	1.9(8)E-3	(E2M1)
387.80	0.42(11)	E0M1	2064.90	1.1(4)E-2	(E0)M1
411.116	1.92(23)E-2	E2	2069.00	7.5(17)E-4	M1(E2)
432.5	>237(24)	E0	2076.21	d	E2M1
493.81	d	E0M1;-	2078.63	d	E2M1
496.37	d	-;E0M1	2082.22	d	E1E2
526.85	8.2(9)E-2	E0M1	2086.20	d	M1E2
543.58	d	(E0M1);-	2093.51	1.25(24)E-3	(M1)
547.47	d	-;(E0M1)	2103.54	6.0(14)E-4	E2(M1)
586.27	2.02(21)E-2	(E0)M1	2113.70	7.0(17)E-4	M1(E2)
615.6	>437(25)	E0	2118.66	1.0(4)E-3	M1
622.79	1.09(17)E-2	E2M1	2150.85	6.6(12)E-4	M1(E2)
675.01	6.0(15)E-3	E2	2158.72	5.4(18)E-4	E2(M1)
678.61	7.4(29)E-3	E2(M1)	2169.15	5.6(13)E-4	E2M1
697.20	d	(E0M1);-	2179.42	d	M1
699.25	d	-;(E0M1)	2182.10	d	M1
702.98	d	E2;M1	2185.24	5.8(17)E-4	E2M1
703.46	d	E2;E1	2196.20	1.01(29)E-3	M1
764.89	5.7(13)E-3	E2M1	2211.7	>3(1)E-2	(E0(M1))
778.904	1.48(24)E-3	E1	2217.40	d	M1
855.00	d	(E0)M1;-	2220.81	d	M1
857.33	d	-;(E0M1)	2251.41	d	M1;-
893.34	7.3(11)E-3	M1	2254.54	d	E1;E2M1
928.43	3.7(18)E-3	E2M1	2275.01	d	(M1)
930.58	4.0(8)E-3	E2M1	2276.87	d	(M1)
953.07	5.6(8)E-3	M1	2289.66	d	(E0)M1
970.32	1.4(5)E-3	E1	2291.46	d	(E0)M1
974.05	5.0(6)E-3	M1	2322.30	d	(E0)M1;-
990.19	1.9(5)E-3	E2	2324.32	d	-;(E0)M1
1010.60	5.7(14)E-3	M1	2342.57	1.32(26)E-3	(E0)M1
1047.9	>2.06(20)	E0	2357.0	>4.0(10)E-2	E0(M1)
1061.6	>8.4(9)E-2	E0(M1)	2365.13	1.2(3)E-3	E0M1
1089.737	2.7(5)E-3	E2M1	2375.34	7.9(18)E-4	M1
1109.19	2.3(4)E-3	E2M1	2384.94	d	(E0)M1;-
1137.56	3.0(6)E-3	M1	2388.72	d	-;(E0)M1
1185.73	1.2(4)E-3	E2(E1)	2398.53	1.9(7)E-3	(E0)M1
1205.83	2.5(11)-3	E1(E2)	2405.00	3.2(9)E-4	E1(E2)
1209.03	4.9(21)E-4	E1	2428.36	2.7(9)E-3	(E0)M1
1261.32	2.2(4)E-3	M1	2465.50	>1.0(3)E-2	E0(M1)
1299.140	5.9(11)E-4	E1	2491.4	>5.0(10)E-2	E0(M1)
1314.20	t	(E1)	2495.53	6.5(27)E-4	M1(E2)
1314.25	t	(E1)	2506.3	>1.0(4)E-2	(E0(M1))
1316.32	t	(E1)	2518.42	5.0(9)E-4	M1(E2)
1318.24	3.1(6)E-3	M1	2523.92	5.1(10)E-4	M1(E2)
1325.86	1.6(4)E-3	E2(M1)	2536.30	6.4(12)E-4	M1
1343.0	>8.0(8)E-2	E0(M1)	2551.48	5.0(13)E-4	M1(E2)

1348.15	1.20(22)E-3	E2	2569.85	3.0(6)E-4	(E1)
1352.98	1.9(4)E-2	E0M1	2588.36	6.2(11)E-4	(M1)
1360.43	d	(E0)M1;-	2600.69	d	E2M1
1363.39	d	-;(E0)M1	2602.85	d	M1E2
1369.04	2.6(7)E-3	M1	2619.61	4.7(9)E-4	M1(E2)
1372.04	1.9(5)E-3	M1(E2)	2655.29	4.1(12)E-4	E2M1
1383.5	>7(1)E-2	E0(M1)	2662.55	2.8(13)E-4	E1E2
1406.16	1.2(5)E-3	E2(M1)	2668.13	5.1(19)E-4	E2M1
1410.73	d	E2M1	2678.03	d	E2M1
1411.48	d	E1	2680.88	d	M1
1446.43	1.3(3)E-3	E2(M1)	2694.48	1.0(20)E-3	(E0)M1
1489.60	2.2(8)E-3	M1(E2)	2697.99	5.3(10)E-4	M1E2
1495.44	4.7(9)E-3	E0M1	2702.98	4.5(18)E-4	E2M1
1506.90	2.7(5)E-3	(E0)M1	2709.47	2.7(8)E-4	E1(E2)
1517.77	d	M1	2719.61	3.7(11)E-4	E2E1
1518.37	d	E2M1	2734.06	2.5(5)E-4	E1
1532.75	1.8(5)E-3	M1	2740.93	9.4(30)E-4	(E0)M1
1562.45	2.3(10)E-3	M1	2744.10	1.2(5)E-4	E1
1586.22	4.5(9)E-4	E1	2754.70	4.1(9)E-4	E2M1
1596.85	1.01(23)E-3	E2E1	2778.28	4.6(10)E-4	M1E2
1605.57	d	E1(E2)	2787.86	2.9(10)E-4	E2M1
1605.99	d	E1(E2)	2793.27	d	M1E2
1631.42	1.07(21)E-3	E2M1	2795.92	d	E2
1640.08	2.1(9)E-3	M1	2808.61	2.0(8)E-4	E1
1663.67	7.3(24)E-3	E0M1	2820.43	3.7(11)E-4	E2M1
1667.38	1.30(24)E-3	M1	2833.50	7(4)E-4	(M1)
1727.72	1.8(4)E-3	M1	2838.15	2.8(9)E-4	E2(M1)
1735.8	>4.2(7)E-2	E0(M1)	2859.06	d	E2M1
1739.46	1.35(30)E-3	M1	2861.75	d	E1
1757.42	6.3(13)E-4	E2	2869.24	4.6(7)E-4	M1
1761.22	6.2(19)E-3	E2(E1)	2878.0	>5.0(9)E-3	E0(M1)
1771.43	1.41(27)E-3	M1	2882.39	2.6(6)E-4	E1
1778.78	1.6(4)E-3	M1	2887.51	d	E2M1
1789.17	d	M1E2	2893.15	d	E2M1
1789.20	d	M1	2902.0	>7.0(23)E-3	(E0(M1))
1798.45	9.2(4)E-4	E2M1	2906.48	1.9(5)E-4	E1
1818.56	1.6(6)E-3	M1	2914.42	9(4)E-4	(M1)
1841.16	d	M1;E2	2918.41	d	E2M1
1841.83	d	E2;M1	2921.85	d	E2M1
1857.48	7.6(28)E-4	E2M1	2927.29	2.9(12)E-4	E2M1
1861.94	8.5(24)E-4	E2M1	2936.0	>5.0(12)E-3	(E0(M1))
1870.55	d	(E0)M1;-	2940.75	3.9(11)E-4	E2M1
1875.35	d	-;(E0)M1	2950.50	3.3(9)E-3	E0M1
1886.08	3.6(11)E-3	(E0)M1			

Note: d(t) – double(triple) transition

Table 8: Multipolarities of double transitions from the ^{152}Tb$\longrightarrow$ ^{152}Gd decay

703.46 keV	$I_K(703.46)_{calc}$		
	E1	E2	M1
702.98 keV	4.279	10.994	20.606
$I_K(702.98)_{calc}$			
E1 2.419	6.699	13.414	23.025
E2 6.216	10.495	<u>17.210</u>	26.822
M1 11.651	<u>15.930</u>	22.645	32.256
I_K(702.98+703.46)=17.3(17)			
1106.59 keV	$I_K(1106.59)_{calc}$		
	E1	E2	M1
1109.20 keV	0.570	1.332	2.220
$I_K(1109.20)_{calc}$			
E1 3.772	4.342	5.104	5.992
E2 8.813	9.383	<u>10.144</u>	<u>11.032</u>
M1 14.688	15.258	16.020	16.907
I_K(1106.59+1109.20)=10.9(11)			
1185.73 keV	$I_K(1185.73)_{calc}$		
	E1	E2	M1
1188.37 keV	0.281	0.647	1.054
$I_K(1188.37)_{calc}$			
E1 0.047	0.328	0.693	1.101
E2 0.108	<u>0.389</u>	0.754	1.162
M1 0.176	<u>0.457</u>	0.822	1.230
I_K(1185.73+1188.37)=0.48(10)			
1261.32 keV	$I_K(1261.32)_{calc}$		
	E1	E2	M1
1263.84 keV	1.062	2.411	3.847
$I_K(1263.84)_{calc}$			
E1 0.082	1.144	2.493	3.929
E2 0.187	1.248	2.597	<u>4.034</u>
M1 0.298	1.360	2.709	<u>4.145</u>

I_K(1261.32+1263.84)=3.64(35)			
1411.48 keV	$I_K(1411.48)_{calc}$		
	E1	E2	M1
1410.73 keV	0.419	0.933	1.415
$I_K(1410.73)_{calc}$			
E1 0.203	0.622	1.136	1.619
E2 0.453	0.872	1.386	1.868
M1 0.687	1.106	1.620	2.102
I_K(1411.48+1410.73)=0.97(14)			
1605.57 keV	$I_K(1605.57)_{calc}$		
	E1	E2	M1
1605.99 keV	0.173	0.376	0.541
$I_K(1605.99)_{calc}$			
E1 0.116	0.290	0.492	0.658
E2 0.252	0.426	0.628	0.793
M1 0.363	0.537	0.739	0.905
I_K(1605.57+1605.99)=0.29(7)			
2018.09 keV	$I_K(2018.09)_{calc}$		
	E1	E2	M1
2020.67 keV	0.010	0.021	0.028
$I_K(2020.67)_{calc}$			
E1 0.006	0.017	0.028	0.034
E2 0.013	0.024	0.034	0.041
M1 0.018	0.028	0.039	0.045
I_K(2018.09+2020.67)=0.047(10)			
2600.69 keV	$I_K(2600.69)_{calc}$		
	E1	E2	M1
2602.85 keV	0.010	0.020	0.024
$I_K(2602.85)_{calc}$			
E1 0.023	0.033	0.043	0.047
E2 0.045	0.055	0.065	0.068
M1 0.053	0.063	0.073	0.076
I_K(2600.69+2602.85)=0.076(9)			

Table 9: Multipolarities of the triple transitions from ^{152}Tb$\longrightarrow$ ^{152}Gd decay

I_K(1518.37,E1)=0.095			
1517.77 keV	$I_K(1517.77)_{calc}$		
	E1	E2	M1
1517.77a keV	0.436	0.958	1.414
$I_K(1517.77b)_{calc}$			
E1 0.027	0.559	1.081	1.537
E2 0.060	0.592	1.113	1.569
M1 0.088	0.620	1.142	1.598
I_K(1518.37,E2)=0.210			
1517.77 keV	$I_K(1517)_{calc}$		
	E1	E2	M1
1517.77a keV	0.436	0.958	1.414
$I_K(1517.77b)_{calc}$			
E1 0.027	0.673	1.195	1.651
E2 0.060	0.706	1.228	1.683
M1 0.088	0.734	1.256	1.712
I_K(1518.37,M1)=0.309			
1517.77 keV	$I_K(1517)_{calc}$		
	E1	E2	M1
1517.77a keV	0.436	0.958	1.414
$I_K(1517.77b)_{calc}$			
E1 0.027	0.773	1.295	1.751
E2 0.060	0.805	1.327	1.783
M1 0.088	0.834	1.356	1.812
I_K(1517.77a+1517.77b+1518.37)=1.77(14)			
I_K(1598.90,E1)=0.173			
1596.86 keV	$I_K(1596.86)_{calc}$		
	E1	E2	M1
1596.53 keV	0.239	0.518	0.750
$I_K(1596.53)_{calc}$			
E1 0.122	0.534	0.813	1.045

E2 0.263	0.675	<u>0.954</u>	1.187
M1 0.088	<u>0.793</u>	1.072	1.305
I_K(1598.90,E2)=0.375			
1596.86 keV	$I_K(1596.86)_{calc}$		
	E1	E2	M1
1596.53 keV	0.239	0.518	0.750
$I_K(1596.53)_{calc}$			
E1 0.122	<u>0.735</u>	1.014	1.247
E2 0.263	<u>0.877</u>	1.156	1.389
M1 0.088	0.995	1.274	1.507
I_K(1598.90,M1)=0.543			
1596.86 keV	$I_K(1596.86)_{calc}$		
	E1	E2	M1
1596.53 keV	0.239	0.518	0.750
$I_K(1596.53)_{calc}$			
E1 0.122	<u>0.904</u>	1.183	1.415
E2 0.263	1.045	1.325	1.557
M1 0.088	1.164	1.443	1.675
I_K(1598.90+1596.86+1596.53)=0.85(12)			

Table 10: Possible contributions to I_K of the (E0+M1) transitions from L, M, and N conversion lines belonging to other transitions

E_γ(E0+M1) keV I_K	$\sigma(E_K)$ keV	E_L,kev I_γ I_L	E_M,kev I_γ I_M	E_N,kev I_γ I_N	$\sum I_i$	$[\sum I_i]$
387.80 242(52)	2.2	345.937 [10000(250)] [663]	339.449 <1.0 <0.018	337.944 <1.0 <0.0042	<0.022	[663]
432.5 703(70)	2.5	390.637 1.17(19) <0.066	384.149 1.9(6) <0.024	382.644 0.88(22) <0.0027	<0.093	
493.81 d17.2(9)	2.8	451.947 1.17(28) <0.044	445.459 <0.8 <0.0067	443.954 <0.8 <0.0016	<0.053	
496.37 d17.2(9)	2.8	454.507 1.17(28) <0.044	448.019 0.8 <0.0067	446.514 0.8 <0.0016	<0.053	
526.85 33.4(17)	2.9	484.987 [9.14(23)] [0.29]	478.499 <0.8 <0.0057	476.994 <0.9 <0.0015	<0.0072	[0.29]
543.58 d10.4(17)	3.0	501.717 1.02(16) <0.030	495.229 [45.3(9)] [0.29]	493.724 [45.3(9)] [0.071]	<0.036	[0.68]
547.47 d10.4(17)	3.0	505.607 [10.16(27)] [0.29]	499.119 1.02(16) <0.0065	497.614 [23.0(5)] [0.035]	<0.036	[0.68]
586.27 291(14)	3.2	544.407 [30.3(7)] [0.72]	537.919 <0.9 <0.0047	536.414 [8.25(20)] [0.010]	<0.0047	[0.73]
615.6 1732(100)	3.4	573.737 2.48(15) <0.058	567.249 1.22(16) <0.0056	565.744 <0.8 <0.00089	<0.064	
699.25 d2.6(5)	3.8	657.387 [9.55(40)] [0.14]	650.899 1.27(12) <0.0041	649.394 1.27(12) <0.00099	<0.0051	[0.14]

699.25 d2.6(5)	3.8	657.387 [9.55(40)] [0.14]	650.899 1.27(12) <0.0041	649.394 1.27(12) <0.00099	<0.0051	[0.14]
855.00 d4.0(9)	4.5	813.137 1.55(18) <0.013	806.649 3.24(14) <0.0062	805.144 3.24(14) <0.0015	<0.021	
857.33 d4.0(9)	4.7	815.467 5.5(5) <0.048	808.979 4.79(25) <0.0091	807.474 4.79(25) <0.0022	<0.059	
1047.9 31.2(31)	2.8	1006.037 0.99(15) <0.0060	999.549 3.24(18) <0.0043	998.044 3.24(18) <0.00021	<0.011	
1061.6 1.56(17)	2.9	1019.737 2.01(13) <0.012	1013.249 [63.2(13)] [0.08]	1011.744 [63.2(13)] [0.019]	<0.012	[0.10]
1343.0 1.39(14)	3.5	1301.137 [325(7)] [1.06]	1294.649 <0.6 <0.0004	1293.144 <0.6 <0.0001	<0.0005	[1.06]
1352.98 1.04(10)	3.5	1311.117 1.50(14) <0.0048	1304.629 <0.6 <0.0004	1303.124 <0.6 <0.0001	<0.0053	
1360.43 d0.62(12)	3.5	1318.567 [73(3)] [0.23]	1312.079 [222(5)] [0.15]	1310.574 1.50(14) <0.00025	<0.00025	[0.38]
1363.39 d0.62(12)	3.6	1321.527 [42.0(17)] [0.13]	1315.039 [73(3)] [0.050]	1313.534 [222(5)] [0.037]		[0.22]
1383.5 0.87(12)	3.6	1341.637 1.93(26) <0.0059	1335.149 1.93(26) <0.0013	1333.644 [19.6(4)] [0.0031]	<0.0072	[0.010]
1495.44 0.90(10)	3.8	1453.577 6.44(30) <0.016	1447.089 1.84(21) <0.0010	1445.584 <0.6 <0.0001	<0.017	

1506.9 0.249(26)	3.9	1465.037 0.68(22) <0.0017	1458.549 6.44(30) <0.0035	1457.044 6.44(30) <0.0008	<0.0060	
1663.67 0.57(14)	4.2	1621.807 5.59(27) <0.01087	1615.319 8.25(28) <0.00347	1613.814 10.73(28) <0.00108	<0.01542	
1735.8 0.145(23)	4.4	1693.937 5.7(13) <0.01	1687.449 6.80(13) <0.0026	1685.944 3.74(12) <0.0003	<0.0129	
1870.55 d0.211(42)	4.7	1828.687 [9.26(28)] [0.014]	1822.199 [23.8(5)] [0.008]	1820.694 [33.1(6)] [0.0025]		[0.0245]
1875.35 d0.211(42)	4.7	1833.487 <0.53 <0.0008	1826.999 [23.8(5)] [0.008]	1825.494 [23.8(5)] [0.0018]	<0.0008	[0.0098]
1886.08 0.19(4)	4.7	1844.217 2.27(11) <0.0033	1837.729 [12.3(3)] [0.0038]	1836.224 <0.53 <0.00004	<0.00334	[0.0038]
1944.8 0.17(6)	4.8	1902.937 [272.1(5)] [0.37]	1896.449 5.3(4) <0.00154	1894.944 5.3(4) <0.0004	<0.00194	[0.37]
1962.9 0.104(43)	4.9	1921.037 5.14(13) <0.00676	1914.549 5.14(13) <0.00146	1913.044 5.14(13) <0.0004	<0.00862	
2014.48 0.088(23)	5.0	1972.617 0.89(13) <0.0011	1966.129 3.30(14) <0.0009	1964.624 3.30(14) <0.0002	<0.0022	
2029.5 0.043(17)	5.0	1987.637 0.75(15) <0.0009	1981.149 [23.97(39)] [0.0063]	1979.644 [23.97(39)] [0.0015]	<0.0009	[0.0078]
2064.9 0.157(43)	5.1	2023.037 1.90(11) <0.00222	2016.549 3.08(23) <0.0008	2015.044 1.18(23) <0.00007	<0.00309	
2211.7 0.104(35)	5.4	2169.837 4.94(17)	2163.349 5.11(24)	2161.844 5.11(24)		

		<0.00494	<0.0011	<0.0003	<0.00634	
2291.46	5.6	2249.597	2243.109	2241.604		
0.345(69)		[24.68(43)]	1.18(13)	1.18(13)		
		[0.023]	<0.00023	<0.00006	<0.00029	[0.023]
2322.30	5.7	2280.437	2273.949	2272.444		
d0.191(35)		7.77(25)	6.24(25)	6.24(25)		
		<0.00694	<0.00121	<0.0003	<0.00845	
2324.32	5.7	2282.457	2275.969	2274.464		
d0.191(35)		5.58(25)	7.77(22)	6.24(25)		
		<0.00498	<0.0015	<0.0003	<0.00678	
2342.57	5.7	2300.707	2294.219	2292.714		
0.312(35)		[4.22(13)]	1.24(12)	1.73(12)		
		[0.0037]	<0.00023	<0.00008	<0.00031	[0.0037]
2357.0	5.7	2315.137	2308.649	2307.144		
0.139(35)		5.9(14)	4.87(14)	4.87(14)		
		<0.0051	<0.0009	<0.00022	<0.00622	
2365.13	5.8	2323.267	2316.779	2315.274		
0.78(14)		1.43(29)	7.3(29)	5.9(14)		
		<0.00123	<0.00135	<0.00026	<0.00284	
2384.94	5.8	2343.077	2336.589	2335.084		
d0.242(24)		[24.7(4)]	1.42(8)	1.42(8)		
		[0.021]	<0.00026	<0.00006	<0.00032	[0.021]
2388.72	5.8	2346.857	2340.369	2338.864		
d0.242(24)		2.3(14)	1.42(8)	1.42(8)		
		<0.00193	<0.00026	<0.00006	<0.00225	
2398.53	5.8	2356.667	2350.179	2348.674		
0.191(52)		2.61(16)	1.42(8)	4.91(16)		
		<0.00217	<0.00025	<0.00021	<0.00263	
2428.36	5.9	2386.497	2380.009	2378.504		
0.294(69)		5.95(14)	2.15(14)	2.15(14)		
		<0.0048	<0.00037	<0.00009	<0.00526	
2465.50	6.0	2423.637	2417.149	2415.644		
0.35(10)		0.87(9)	1.68(10)	1.68(9)		
		<0.00068	<0.00028	<0.00007	<0.00103	

2491.4 0.173(35)	6.0	2449.537 1.75(11) <0.00133	2443.049 2.77(11) <0.00045	2441.544 2.77(11) <0.00011	<0.00189	
2506.3 0.035(15)	6.1	2464.437 2.22 <0.0017	2457.949 0.77 <0.00013	2456.444 0.77 <0.00003	<0.00186	
2694.48 0.095(10)	6.5	2652.617 8.72(25) [0.006]	2646.129 2.71(17) <0.00037	2644.624 2.71(17) <0.00009	<0.00046	[0.006]
2740.93 0.043(12)	6.5	2699.067 [45.8(7)] [0.028]	2692.579 [38.4(7)] [0.005]	2691.074 [10.44(24)] [0.0003]		[0.0333]
2878.0 0.016(3)	6.9	2836.137 [5.56(9)] [0.0031]	2829.649 0.68(6) <0.00008	2828.144 0.68(6) <0.000019	<0.000099	[0.0031]
2902.0 0.024(8)	6.9	2860.137 3.25(10) <0.00176	2853.649 3.25(10) 0.0004	2852.144 <0.24 <0.00007	<0.00223	
2936.0 0.017(6)	7.0	2894.137 2.43(8) <0.00128	2887.649 2.43(8) <0.00028	2886.144 2.43(8) <0.00007	<0.00163	
2950.50 0.019(3)	7.0	2908.637 0.38(6) <0.0002	2902.149 [7.22(23)] [0.0008]	2900.644 [7.22(23)] [0.0002]	<0.0002	[0.001]

Table 11: Rasmussen parameters X for the transitions with E0 admixtures

E_γ, keV	q_1^2	X_1	q_2^2	X_2	Placement
387.80	18(4)	0.36(8)	34(8)	0.70(17)	$1318, 2^+ \rightarrow 930, 2^+$
d496.37	5.5(4)	0.168(14)	10.1(9)	0.308(27)	$1605, 2^+ \rightarrow 1109, 2^+$
526.85	7.2(6)	0.242(19)	13.5(11)	0.45(4)	$1282, 4^+ \rightarrow 755, 4^+$
d543.58	2.7(6)	(0.098(23))	4.6(13)	(0.16(5))	$1862, 2^+ \rightarrow 1318, 2^+$
586.30	1.68(12)	0.068(5)	—	—	
1061.6	> 39	> 4.8	> 78	> 9	
1343.0	64(34)	12(6)	128(68)	24(13)	$3285, 2^+ \rightarrow 1941, 2^+$
1352.98	14.2(25)	2.7(5)	28(5)	5.3(10)	$2667, 1^- \rightarrow 1314, 1^-$
1383.5	60(30)	12(6)	120(64)	24(13)	
1495.44	3.5(6)	0.80(15)	6.4(13)	1.5(3)	$1839, 2^+ \rightarrow 344, 2^+$
1506.90	1.6(4)	(0.38(8))	2.8(7)	(0.65(17))	$3112, 2^+ \rightarrow 1605, 2^+$
1663.67	7.4(22)	2.1(6)	14(4)	4.1(13)	$2772, 2^+ \rightarrow 1109, 2^+$
1735.8	> 51	> 16	> 102	> 31	$3285, 2^+ \rightarrow 1550, 2^+$
1870.55	21(6)	(7.3(19))	41(11)	(15(4))	
1886.08	4.2(12)	(1.5(4))	8(2)	(2.8(9))	$2641, 4^+ \rightarrow 755, 4^+$
1944.8	> 74	(> 28)	> 148	(> 56)	$3067, 3^- \rightarrow 1123, 3^-$
1962.9	> 46	(> 18)	> 91	(> 35)	
2014.48	10(4)	(3.8(14))	19(7)	(7.5(28))	
2029.5	> 20	(> 8)	> 39	(> 16)	
2064.90	18(6)	(7.4(25))	35(12)	(15(5))	
d2324.32	5.4(13)	(2.8(7))	11(3)	(5.5(14))	$3079, 4^+ \rightarrow 755, 4^+$
2342.57	1.9(4)	(0.98(21))	3.5(8)	(1.8(4))	$2687, 2^+ \rightarrow 344, 2^+$
2357.0	> 86	> 46	> 171	> 92	
d2384.94	2.2(4)	1.20(22)	4.1(8)	2.3(4)	$2729, 2^+ \rightarrow 344, 2^+$
2398.53	3.3(13)	(1.8(7))	6.3(26)	(3.5(15))	$3328, 2^+ \rightarrow 930, 2^+$
2428.36	5.3(16)	(3.0(9))	10(3)	(5.8(18))	$3357, 2^+ \rightarrow 930, 2^+$
2491.4	> 118	> 70	> 236	> 140	
2694.48	1.9(4)	(1.29(26))	3.6(8)	(2.5(5))	$3310, (1, 2^+) \rightarrow 615, 0^+$
2740.93	1.7(8)	(1.2(6))	3.2(16)	(2.3(11))	$3085, 2^+ \rightarrow 344, 2^+$
2878.0	> 13	> 10	> 26	> 20	
2902.0	> 21	(> 16)	> 41	(> 32)	
2936.0	> 15	(> 12)	> 29	(> 23)	$3550, 0^+ \rightarrow 615, 0^+$
2950.50	9.7(23)	7.9(19)	19(5)	16(4)	

References

[1] J.Adam et al. Izv. AN SSSR, ser.fiz, 34(1970)813 .

[2] D.R.Zolnowski, E.G.Funk, J.W.Mihelich Nucl.Phys. A177(1971)513.

[3] J.Frana Acta Polytechnika, 1998, v.38 No.3, p.127.

[4] Nuclear Decay Schemes, ed. Firestone, 8-th edition.

[5] Gamma and X-ray spectroscopy with semiconductor detectors, R.G.Helmer, H.Debertin, North-Holland, 1989.

[6] J.Adam et al. In: Proceedings of 48 Meeting on Nuclear Spectroscopy and Structure of Atomic Nuclei, St-Petersburg, 1998, p.318.

[7] K.Ya.Gromov et al. Nucl.Phys. A99(1967)585-604.

[8] F.Rossel Atomic Data and Nuclear Data Tables, 21(1978)290.

[9] J.Adam et al. JINR Communication, P6-86-394, Dubna, 1986.

[10] R.S.Hager, E.C.Seltser Nuclear Data Tables A6(1969)1.

[11] D.A.Bell et al. Can.J.Phys. 48(1970)2542.

[12] N.R.Johnson et al. Phys.Rev. C26(1982)1004.

[13] C.A.Kalfas et al. Nucl.Phys. A196(1972)615.

[14] K.Heyde, R.A.Meyer Phys.Rev. C37(1988)2170.

[15] J.Kantele Preprint RR18/81, University of Jyväskylä, 1981.

Received by Publishing Department
on April 28, 2001.

Адам И. и др. E6-2001-93
Гамма-лучи и E0- и M1+E0-переходы в распаде ^{152}Tb $\rightarrow$ ^{152}Gd

Распад ^{152}Tb исследовался с помощью измерения простых γ-спектров. Наблюдалось 704 перехода, из которых 347 мы приписали к распаду ^{152}Tb впервые. Получены более точные и полные данные по интенсивностям γ-переходов. С использованием ранее опубликованных данных по интенсивностям конверсионных электронов были определены E0- или E0+M1-мультипольности для ряда переходов.

Работа выполнена в Лаборатории ядерных проблем им. В.П.Джелепова ОИЯИ.

Сообщение Объединенного института ядерных исследований. Дубна, 2001

Adam J. et al. E6-2001-93
Gamma-Rays and E0 and M1+E0 Transitions
in ^{152}Tb $\rightarrow$ ^{152}Gd Decay

The decay of ^{152}Tb has been investigated by means of measurements of single γ-spectra. The 704 transitions were observed, of which 347 were identified to the decay of ^{152}Tb for the first time. Using the more precise and full data about intensities of γ-transitions and previously reported conversion electron intensities the E0 or M1+E0 multipolarities were established for several transitions.

The investigation has been performed at the Dzhelepov Laboratory of Nuclear Problems, JINR.

Communication of the Joint Institute for Nuclear Research. Dubna, 2001

Макет Т.Е.Попеко

Подписано в печать 26.06.2001
Формат 60 × 90/16. Офсетная печать. Уч.-изд. л. 2,73
Тираж 320. Заказ 52736. Цена 3 р. 25 к.

Издательский отдел Объединенного института ядерных исследований
Дубна Московской области